Compressible Boundary Layer Stability Analysis With Parabolized Stability Equations

Gao Bing[1], Park.S.O.[2]

Department of Aerospace Engineering, School of Mechanical and Aerospace Systems, KAIST

An accurate and cost efficient method PSE is used for the stability analysis of 2D or 3D compressible boundary layers. A highly accurate finite difference PSE code has been developed at a general curvilinear coordinate system using an implicit marching procedure to deal with a broad range of transition predictions problems. Evolution of disturbances in compressible flat plate boundary layers are studied for free-stream Mach numbers ranging from 0 to 1.5. The effect of mean-flow nonparallelism is found to be weak on two dimensional waves and strong on three dimensional waves. The maximum amplification rate increases monotonically with Mach number. The present PSE solutions are compared with previous numerical investigations and experimental results and are found to be in good agreement.

Keywords: Parabolized stability equations, Stability, Non-orthogonal coordinate system, Nonparallel effect, Compressible boundary layers, Implicit marching procedure

1. Introduction

The subject of compressible boundary-layer stability has attracted a great deal of interest in the past few years due to its importance in understanding the onset of transition in high-speed flows and providing some theoretical background for laminar flow control techniques[1]. The objective of the present work is the development of an accurate and cost efficient way for investigating the stability of 2D or 3D boundary layers such as flat plate, finite wings, cone, or bodies at angle of attack.

Most investigations of compressible linear stability have employed what is known as the "quasi-parallel" approach whereby the growth of the boundary layer is ignored and the linear Navier-Stokes equations are reduced to ordinary differential equations by assuming a wave-like disturbance of the form. The linear ODE's along with the homogeneous boundary conditions constitute an eigenvalue problem, which can be solved by standard eigenvalue techniques. For a given flow, this eigenvalue approach can be applied "locally" at various locations along the body in order to obtain an idea about overall growth of disturbances and to correlate with transition location using empirical method, such as e^N method. But its usefulness is limited by inaccuracies due to the parallel flow approximation. Another limitation is that the assumption of local parallel flow which cuts the physical connection between the disturbances at different locations and introduces ambiguity in the calculation of N factors. Different strategies have been employed to reconnect the solution at different locations[2][3],and evaluations of their merits are still inconclusive.

Another transition prediction tool is the direct numerical simulations (DNS) using full Navier-Stokes equations. But it requires far too much computer power. Moreover, they have been obtained only for very simple geometries such as flat

1 Phd student, Aerospace Engineering ,KAIST
2 Professor, Aerospace Engineering ,KAIST
* Corresponding author E-mail: gaobing@sop1.kaist.ac.kr

plate. Therefore, it is not appropriate for studying the transition over the complex geometries[4].

With the introduction of the PSE concept by Herbert, Bertolotti and Chang, it become possible to directly track physically connected disturbances along the marching direction with little computer power over the complex geometries.

2 Problem Formulations

2.1 Disturbance equations

Both the compressible linear stability equations (LST) and the parabolized stability equations (PSE) originate from the compressible Navier-Stokes equations. The gas is assumed to be perfect Newtonian gas. The three dimensional Navier-Stokes equations in Cartesian (x^*,y^*,z^*) coordinate ,where * denotes dimensional quantities, are [5]

$$\frac{\partial \rho^*}{\partial t^*}+\nabla\cdot(\rho^* u^*)=0 \tag{1}$$

$$\rho^*[\frac{\partial u^*}{\partial t^*}+u^*\nabla u^*]=-\nabla p^*+\nabla\cdot[\lambda^*(\nabla\cdot u^*)I+\mu^*(\nabla u^*+\nabla u^{*tr})] \tag{2}$$

$$\rho^* c_p^*[\frac{\partial T^*}{\partial t^*}+u^*\cdot\nabla T^*]=\nabla\cdot(k^*\nabla T^*)+\frac{\partial p^*}{\partial t^*}+u^*\cdot\nabla u^*+\Phi^* \tag{3}$$

$$p^*=\rho^* R^* T^* \tag{4}$$

where u^* is the velocity vector, ρ^* is the density, p^* is the pressure, T^* is the temperature, R^* is the gas constant, c_p^* is the specific heat at constant pressure, k^* is the thermal conductivity, μ^* is the first coefficient of viscosity, and λ^* is the second coefficient of viscosity. The viscous dissipation function, Φ^* is given as

$$\Phi^*=\lambda^*(\nabla\cdot u^*)^2+\frac{\mu^*}{2}(\nabla u^*+\nabla u^{*tr}) \tag{5}$$

First we use Cartesian coordinate system (x^*,y^*,z^*). All the lengths are assumed scaled by a reference length $L^*=\sqrt{\nu_\infty^* x_\infty^*/u_\infty^*}$, velocity by u_∞^*, density by ρ_∞^*, pressure by $\rho_\infty^* u_\infty^{*2}$, and time by L^*/u_∞^* and other variables by their corresponding boundary layer edge values. The instantaneous non-dimensional values of velocities, u,v,w, pressure p, temperature T, density ρ, may be represented as

$$\begin{aligned} &u=\overline{U}+\tilde{u};v=\overline{V}+\tilde{v};w=\overline{W}+\tilde{w}\\ &p=\overline{P}+\tilde{p};T=\overline{T}+\tilde{T};\rho=\overline{\rho}+\tilde{\rho}\\ &\mu=\overline{\mu}+\tilde{\mu};\lambda=\overline{\lambda}+\tilde{\lambda};k=\overline{k}+\tilde{k}\end{aligned} \tag{6}$$

Substituting (6) into the non-dimensional form of the governing equations yields the linearized perturbation equations.

$$\begin{aligned} &\Gamma\frac{\partial\phi}{\partial t}+A\frac{\partial\phi}{\partial x}+B\frac{\partial\phi}{\partial y}+C\frac{\partial\phi}{\partial z}+D\phi\\ &=V_{xx}\frac{\partial^2\phi}{\partial x^2}+V_{yy}\frac{\partial^2\phi}{\partial y^2}+V_{zz}\frac{\partial^2\phi}{\partial z^2}+\\ &V_{yz}\frac{\partial^2\phi}{\partial y\partial z}+V_{xz}\frac{\partial^2\phi}{\partial x\partial z}+V_{xy}\frac{\partial^2\phi}{\partial x\partial y}\end{aligned} \tag{7}$$

where $\phi=[\tilde{p},\tilde{u},\tilde{v},\tilde{w},\tilde{T}]^{tr}$

The disturbance equations are recast using a completely general transformation of the form, which permits the non-orthogonal coordinate system.

$$\xi=\xi(x,y,z);\eta=\eta(x,y,z);\zeta=\zeta(x,y,z) \tag{8}$$

where ξ,η,ζ are streamwise, normal, and spanwise direction respectively.

Finally, we obtain the disturbance equations in the following form,

$$\begin{aligned} &\overline{\Gamma}\frac{\partial\phi}{\partial t}+\overline{A}\frac{\partial\phi}{\partial\xi}+\overline{B}\frac{\partial\phi}{\partial\eta}+\overline{C}\frac{\partial\phi}{\partial\zeta}+\overline{D}\phi\\ &=\overline{V_{\xi\xi}}\frac{\partial^2\phi}{\partial\xi^2}+\overline{V_{\eta\eta}}\frac{\partial^2\phi}{\partial\eta^2}+\overline{V_{\zeta\zeta}}\frac{\partial^2\phi}{\partial\zeta^2}+\overline{V_{\eta\xi}}\frac{\partial^2\phi}{\partial\eta\partial\zeta}\\ &+\overline{V_{\xi\zeta}}\frac{\partial^2\phi}{\partial\xi\partial\zeta}+\overline{V_{\xi\eta}}\frac{\partial^2\phi}{\partial\xi\partial\eta}\end{aligned} \tag{9}$$

2.2 Full three-dimensional linear PSE equations

Direct solution of the disturbance equations (9) is referred to as the direct numerical simulation (DNS) method. DNS requires a significant amount of computational time even for a simple linear case. Here a more efficient approximate solution to the disturbance equation is more desirable.

The disturbance equations are hyperbolic in time for the convection terms (inviscid part). When we consider only the spatial derivatives, it is elliptic in the streamwise direction due to two reasons. First, the streamwise viscous term $\overline{V_{xx}}$ allows any disturbances to be diffused upstream. Second, and more importantly, the convection term in the streamwise direction makes the upstream propagation of acoustic waves possible. One way to parabolize the disturbance equations and make the marching solution feasible is to neglect the viscous diffusion terms along the streamwise direction and prohibit the upstream wave propagation either by dropping the left-running characteristics or suppressing some part of the streamwise pressure gradient, as it is done in the PNS approach. But direct application of the parabolizing procedure used in the PNS approach for mean flow computations to the disturbance equations would not capture the flow physics due

to the suppression of the wave propagation along the left-running characteristics[6].

For compressible stability problems, the disturbances are essentially unsteady waves propagating across the whole boundary layer and the amplitudes of these waves reach their maxima near the critical layer located between the wall and the boundary layer edge. These instability waves undergo a "fast-oscillation"(phase change") as they evolve along the flow direction. It is valuable to decompose the disturbances into a fast-oscillatory wave part and a slowly varying shape function because we can keep the ellipticity for the wave part while parabolizing the governing equations for the shape function. It is assumed that the disturbance vector Φ, for an instability wave with frequency ω and a spanwise wave number β and a streamwise wave number, can be expressed as

$$\phi(\xi,\eta,\zeta,t)=\Psi(\xi,\eta,\zeta)\exp[i\theta(\xi,\zeta,t)] \tag{10}$$

where

$$\frac{\partial\theta}{\partial t}=-\omega;\alpha(\xi,\zeta)=\frac{\partial\theta}{\partial\xi};\beta(\xi,\zeta)=\frac{\partial\theta}{\partial\zeta} \tag{11}$$

From (11), the wave number must satisfy the irrotational condition.

$$\frac{\partial\alpha}{\partial\zeta}=\frac{\partial\beta}{\partial\xi}=\frac{\partial^2\theta}{\partial\xi\partial\zeta} \tag{12}$$

Substitute (10) and (11) into the equations (9), it gives equation (13)

$$\begin{aligned}&\tilde{D}\phi+\tilde{A}\frac{\partial\phi}{\partial\xi}+\tilde{B}\frac{\partial\phi}{\partial\eta}+\tilde{C}\frac{\partial\phi}{\partial\zeta} \\ &=\overline{V}_{\xi\xi}\frac{\partial^2\phi}{\partial\xi^2}+\overline{V}_{\eta\eta}\frac{\partial^2\phi}{\partial\eta^2}+\overline{V}_{\zeta\zeta}\frac{\partial^2\phi}{\partial\zeta^2}+\overline{V}_{\xi\eta}\frac{\partial^2\phi}{\partial\xi\partial\eta} \\ &+\overline{V}_{\xi\zeta}\frac{\partial^2\phi}{\partial\xi\partial\zeta}+\overline{V}_{\eta\zeta}\frac{\partial^2\phi}{\partial\eta\partial\zeta}\end{aligned} \tag{13}$$

where

$$\begin{aligned}&\tilde{D}=-i\omega\overline{\Gamma}+i\alpha\overline{A}+i\beta\overline{C}+\overline{D}+\overline{V}_{\xi\xi}\alpha^2+\overline{V}_{\xi\zeta}\alpha\beta \\ &\quad+\overline{V}_{\zeta\zeta}\beta^2-i(\overline{V}_{\xi\xi}\frac{\partial\alpha}{\partial\xi}+\overline{V}_{\xi\zeta}\frac{\partial\alpha}{\partial\zeta}+\overline{V}_{\zeta\zeta}\frac{\partial\beta}{\partial\zeta}) \\ &\tilde{A}=\overline{A}-2i\alpha\overline{B}_{\xi\xi}-i\beta\overline{V}_{\xi\zeta} \\ &\tilde{B}=B-i\alpha\overline{V}_{\xi\eta}-i\beta\overline{V}_{\eta\zeta} \\ &\tilde{C}=\overline{C}-i\alpha\overline{V}_{\xi\zeta}-2i\beta\overline{V}_{\zeta\zeta} \\ &\overline{V}_{\xi\eta}=\overline{V}_{\xi\eta};\overline{V}_{\xi\zeta}=\overline{V}_{\xi\zeta};\overline{V}_{\eta\zeta}=\overline{V}_{\eta\zeta} \\ &\overline{V}_{\eta\eta}=\overline{V}_{\eta\eta};\overline{V}_{\xi\xi}=\overline{V}_{\xi\xi};\overline{V}_{\zeta\zeta}=\overline{V}_{\zeta\zeta}\end{aligned}$$

We note here that matrices $\tilde{A},\tilde{B},\tilde{C},\tilde{D}$ have contributions from both inviscid and viscous terms, and thus contain terms of order one and of order $1/R_0$($R_0$is the reference Reynolds number $R_0=u_\infty^*L^*/\nu_\infty^*$).

While matrices $\overline{V}_{\xi\xi},\overline{V}_{\eta\eta},\overline{V}_{\zeta\zeta},\overline{V}_{\xi\eta},\overline{V}_{\xi\zeta},\overline{V}_{\eta\zeta}$ are solely due to viscous diffusion and are of order $O(1/R_0)$.We also assume the shape function is changed slowly along the streamwise direction and spanwise direction , whose derivatives along both directions have an order of $O(1/R_0)$. So after neglecting all the terms, whose orders are $O(1/R_0^2)$, we have

$$\tilde{D}\psi+\tilde{A}\frac{\partial\psi}{\partial\xi}+\tilde{B}\frac{\partial\psi}{\partial\eta}+\tilde{C}\frac{\partial\psi}{\partial\zeta}=\overline{V}_{\eta\eta}\frac{\partial^2\psi}{\partial\eta^2} \tag{14}$$

2.3 Quasi-3D linear PSE equations

If we just consider 2D mean flow, the disturbance will be quasi-3D. So the disturbance vector ϕ can be expressed as

$$\phi(\xi,\eta,\zeta,t)=\psi(\xi,\eta)\exp[i\theta(\xi,\zeta,t)] \tag{15}$$

where

$$\frac{\partial\theta}{\partial t}=-\omega;\frac{\partial\theta}{\partial\xi}=\alpha(\xi);\frac{\partial\theta}{\partial\zeta}=\beta \tag{16}$$

The streamwise wavenumber α is only function of ξ.The spanwise wavenumber β is kept constant when disturbance is marching downstream.

Substitute (15) and (16) into the equations (9), after neglecting all the terms order of $O(1/R_0^2)$ .it gives

$$\tilde{D}\psi+\tilde{A}\frac{\partial\psi}{\partial\xi}+\tilde{B}\frac{\partial\psi}{\partial\eta}=\overline{V}_{\eta\eta}\frac{\partial^2\psi}{\partial\eta^2} \tag{17}$$

where

$$\begin{aligned}&\tilde{D}=-i\omega\overline{\Gamma}+i\alpha\overline{A}+i\beta\overline{C}+\overline{D}+\overline{V}_{\xi\xi}\alpha^2+\overline{V}_{\xi\zeta}\alpha\beta \\ &\quad+\overline{V}_{\zeta\zeta}\beta^2-i\overline{V}_{\xi\xi}\frac{d\alpha}{d\xi} \\ &\tilde{A}=\overline{A}-2i\alpha\overline{B}_{\xi\xi}-i\beta\overline{V}_{\xi\zeta} \\ &\tilde{B}=B-i\alpha\overline{V}_{\xi\eta}-i\beta\overline{V}_{\eta\zeta} \\ &\overline{V}_{\xi\eta}=\overline{V}_{\xi\eta};\overline{V}_{\xi\zeta}=\overline{V}_{\xi\zeta};\overline{V}_{\eta\zeta}=\overline{V}_{\eta\zeta} \\ &\overline{V}_{\eta\eta}=\overline{V}_{\eta\eta};\overline{V}_{\xi\xi}=\overline{V}_{\xi\xi};\overline{V}_{\zeta\zeta}=\overline{V}_{\zeta\zeta}\end{aligned}$$

In this paper, we will concentrate on quasi-3D disturbance and test the characteristic of PSE and make preparation for full-3D stability research on 3D mean flow in the future.

2.4 Boundary conditions

The solution of (14) and (17) requires proper boundary conditions in the wall-normal direction. We apply the homogeneous Dirichlet conditions at wall

$$\hat{u}=0,\ \hat{v}=0,\ \hat{w}=0,\ \hat{T}=0 \quad \text{at } y=0 \tag{18}$$

At the free-stream

$$\hat{u}\to0,\ \hat{v}\to0,\ \hat{w}\to0,\ \hat{T}\to0 \quad \text{at } y\to\infty \tag{19}$$

The temperature boundary condition at wall is reasonable

because the disturbance's frequency is much greater than the thermal response time of the wall.

2.5 The closed Equations of PSE

In the full 3D PSE equation (12) and (14), they include seven unknown quantities $\hat{p},\hat{u},\hat{v},\hat{w},\hat{T},\alpha,\beta$ and only have six equations. In the quasi-3D PSE equations (17), it includes six unknown quantities $\hat{p},\hat{u},\hat{v},\hat{w},\hat{T},\alpha$,and only has five equations when a constant spanwise wave number β and frequency ω are given. So the PSE system is not closed. The hypothesis the PSE is derived is the slowly changed shape function, and its derivative in streamwise and spanwise direction order of $O(1/R_0)$.How to make this hypothesis feasible will constitute the closed equation. Herbert suggested a norm condition that is both physically and mathematically meaningful.

For quasi-3D disturbance, the closed equation is

$$\int_{\Omega}\left(\hat{u}^{\dagger}\frac{\partial\hat{u}}{\partial\xi}+\hat{v}^{\dagger}\frac{\partial\hat{v}}{\partial\xi}+\hat{w}^{\dagger}\frac{\partial\hat{w}}{\partial\xi}\right)d\eta=0 \qquad (20)$$

For full 3D disturbance, it needs another equation at spanwise direction.

$$\int_{\Omega}\left(\hat{u}^{\dagger}\frac{\partial\hat{u}}{\partial\zeta}+\hat{v}^{\dagger}\frac{\partial\hat{v}}{\partial\zeta}+\hat{w}^{\dagger}\frac{\partial\hat{w}}{\partial\zeta}\right)d\eta=0 \qquad (21)$$

This choice makes the total kinetic energy of the shape functions independent of ξ or ζ. The total kinetic energy is

$$E=\int_{\Omega}\left(|\hat{u}|^2+|\hat{v}|^2+|\hat{w}|^2\right)d\eta$$

The growth of the disturbance energy is absorbed into the phase functionθ.

3 Numerical Methods

In the streamwise direction, we use the implicit backward Euler method. In the wall normal direction, we use fourth order finite difference method[5]. The determining factor in choosing the streamwise schemes is stability. In the wall normal direction, because the critical layer moves away from the wall towards the edge of the boundary layer, the grid distributions suitable at certain Mach number must be chosen carefully. In order to avoid to use artificial pressure boundary conditions, we use one-side difference which does not involve the wall points to approximate the first derivative of pressure.

Here we express general quasi-3D PSE equations (17) into computation domain (ξ,η)

$$\underline{D}\phi+\underline{A}\frac{\partial\phi}{\partial\xi}+\underline{B}\frac{\partial\phi}{\partial\eta}=\underline{V}\frac{\partial^2\phi}{\partial\eta^2} \qquad (22)$$

Here, in order to be convenient, we write (22) as

$$D\phi+A\frac{\partial\phi}{\partial\xi}+B\frac{\partial\phi}{\partial\eta}=V\frac{\partial^2\phi}{\partial\eta^2} \qquad (23)$$

The discretized equations can be writtten as

(1) For $J=2$

$$D_{ij}\phi_{ij}+A_{ij}\frac{\phi_{ij}-\phi_{i-1j}}{\Delta\xi}+$$
$$m_1B_{ij}\frac{-3\phi_{ij-1}-10\phi_{ij}+18\phi_{ij+1}-6\phi_{ij+2}+\phi_{ij+3}}{12\Delta\eta}$$
$$+m_2B_{ij}\frac{-25\phi_{ij}+48\phi_{ij+1}-36\phi_{ij+2}+16\phi_{ij+3}-3\phi_{ij+4}}{12\Delta\eta}$$
$$=V_{ij}\frac{10\phi_{ij-1}-15\phi_{ij}-4\phi_{ij+1}+14\phi_{ij+2}-6\phi_{ij+3}+\phi_{ij+4}}{12\Delta\eta^2}$$

(2) For $J=3$

$$D_{ij}\phi_{ij}+A_{ij}\frac{\phi_{ij}-\phi_{i-1j}}{\Delta\xi}+$$
$$m_1B_{ij}\frac{\phi_{ij-2}-8\phi_{ij-1}+8\phi_{ij+1}-\phi_{ij+2}}{12\Delta\eta}$$
$$+m_2B_{ij}\frac{-3\phi_{ij-1}-10\phi_{ij}+18\phi_{ij+1}-6\phi_{ij+2}+\phi_{ij+3}}{12\Delta\eta}$$
$$=V_{ij}\frac{-\phi_{ij-2}+16\phi_{ij-1}-30\phi_{ij}+16\phi_{ij+1}-6\phi_{ij+2}}{12\Delta\eta^2}$$

(3) For $3<J<JM-2$

$$D_{ij}\phi_{ij}+A_{ij}\frac{\phi_{ij}-\phi_{i-1j}}{\Delta\xi}+B_{ij}\frac{\phi_{ij-2}-8\phi_{ij-1}+8\phi_{ij+1}-\phi_{ij+2}}{12\Delta\eta}$$
$$=V_{ij}\frac{-\phi_{ij-2}+16\phi_{ij-1}-30\phi_{ij}+16\phi_{ij+1}-6\phi_{ij+2}}{12\Delta\eta^2}$$

(4) For $J=JM-2$

$$D_{ij}\phi_{ij}+A_{ij}\frac{\phi_{ij}-\phi_{i-1j}}{\Delta\xi}+$$
$$m_1B_{ij}\frac{\phi_{ij-2}-8\phi_{ij-1}+8\phi_{ij+1}-\phi_{ij+2}}{12\Delta\eta}$$
$$+m_2B_{ij}\frac{-\phi_{ij-3}+6\phi_{ij-2}-18\phi_{ij-1}+10\phi_{ij}+3\phi_{ij+1}}{12\Delta\eta}$$
$$=V_{ij}\frac{-\phi_{ij-2}+16\phi_{ij-1}-30\phi_{ij}+16\phi_{ij+1}-\phi_{ij+2}}{12\Delta\eta^2}$$

(5) For $J=JM-1$

$$D_{ij}\phi_{ij}+A_{ij}\frac{\phi_{ij}-\phi_{i-1j}}{\Delta\xi}+$$
$$m_1B_{ij}\frac{-\phi_{ij-3}+6\phi_{ij-2}-18\phi_{ij-1}+10\phi_{ij}+3\phi_{ij+1}}{12\Delta\eta}$$
$$+m_2B_{ij}\frac{3\phi_{ij-4}-16\phi_{ij-3}+36\phi_{ij-2}-48\phi_{ij-1}+25\phi_{ij}}{12\Delta\eta}$$
$$=V_{ij}\frac{\phi_{ij-4}-6\phi_{ij-3}+14\phi_{ij-2}-4\phi_{ij-1}-15\phi_{ij}+10\phi_{ij+1}}{12\Delta\eta^2}$$

where $m_1 = 1$, $m_2 = 0$ for component $\hat{u}$, $\hat{v}$, $\hat{w}$, $\hat{T}$; $m_1 = 0$, $m_2 = 1$ for component $\hat{p}$

Chang et al. pointed out that the PSE equations are only "nearly parabolic"due to the streamwise pressure gradient term inherited form the original Navier- Stokes equation. Numerical instability similar to that observed in PNS will occur if one attempt to solve PSE by using a small enough marching step size[6]. Li and Malik [7] use Fourier analysis to prove the existence of numerical instability and quantify the numerical instability bound, which is that the minimum step size is greater than the inverse of the real part of the streamwise wave number. This step-size restriction can be overcome by dropping the $d\alpha/d\xi$ term from the governing equations. The effect of this term on solution accuracy is negligible for Blasius flow but not so for rotating-disk flow. In order to keep the accuracy of PSE because of removing this term, we can assume $d\alpha/d\xi = 0$ locally and take α as step-function.

The iteration procedure is following,

(1) Assume $d\alpha/d\xi = 0$ at i+1 step

(2) Give a guessed value α_{i+1}, and evaluate PSE coefficient matrix D, A, B, V at i+1 step

(3) Solve the value ϕ_{i+1} using implicit backward Euler scheme.

(4) Update the α_{i+1} using new ϕ_{i+1} based on the closed equations.

(5) Check if $\alpha_{i+1}^{N} - \alpha_{i+1}^{O} < \epsilon$. If yes, $i = i+1$, if no, go back to step 1

4 Mean Flow Computation

In order to verify PSE procedure, the flat plate flow is first tested. The mean flow of flat plate is obtained by the coupled laminar boundary layer code using Falkner-Skan transformation[8],which is suitable for the stability calculation. The code used here is written for large variation of properties and use a fourth order polynomial approximation to get the coefficients of specific heat, viscosity and the conductivity, which was given by least squares interpolation of experimental data between the temperature of 100K and 1600K.

The mean flow is calculated under two conditions: one is that the specific heat c_p is constant; the other is that the specific heat is changed with temperature. It is very obvious that the difference is large as the Mach number is increased.

One can anticipate that in supersonic flows a change in growth rate of ten percent or more due to the thermodynamic approximations could easily pollute the measurements of nonparallel effects. So it is important to get an accurate value of properties especially at high Mach number.

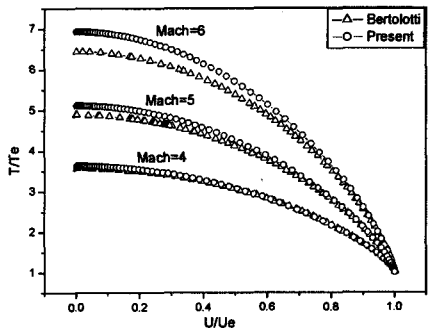

Fig. 4.1 Mean flow calculation at different Mach number at constant specific heat

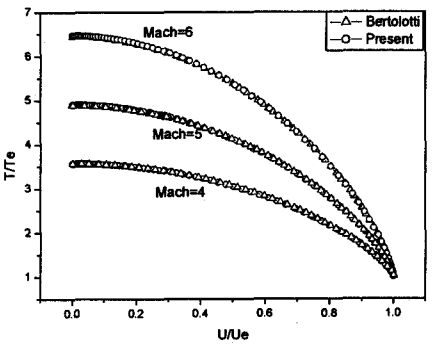

Fig. 4.2 Mean flow calculation at different Mach number at variable specific heat

The following figures will give the profiles of mean flow at M=1.5 calculated by mean flow code.

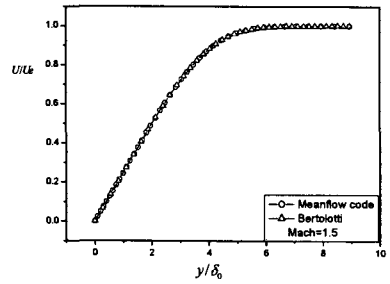

Fig 4.3 Streamwise velocity profile of flat plate at M=1.5

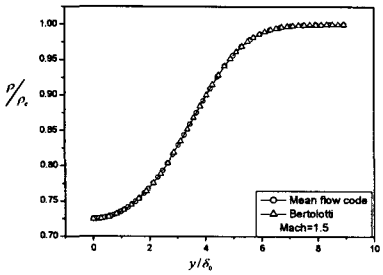

Fig 4.4 Density profile of flat plate at M=1.5

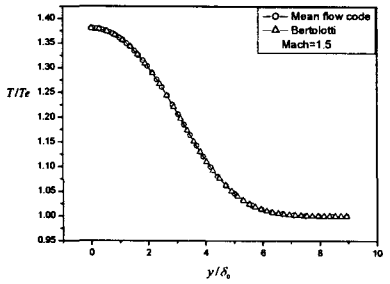

Fig 4.5 Temperature profile of flat plate at M=1.5

5 Initial conditions

We can give the solution obtained under the parallel flow approximation as initial conditions, however, the modification due to the basic-flow non-parallelism is sufficient to cause transients in the marching solution that are objectionably large[9]. We follow the procedure of Bertolotti[9] and expand ϕ, α and mean flow in a Taylor series locally and insert the expansions into PSE equations and closed equations. We then observe that order $O(1)$ and $O(x)$ terms must independently sum to zero and then use Newton-Raphson iteration to solve the initial equations.

In order to test the method, it is first used at the parallel flow calculation to find unstable modes. The present results are seen to be consistent with results of Malik and Bertolotti. The symbol γ denotes the growth rate, α_r denotes the wave number.

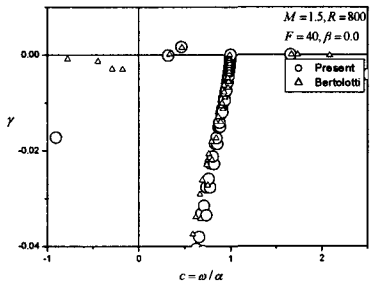

Fig.5.1 Spectrum of eigenvalues, spatial growth, parallel flow,2D disturbance.

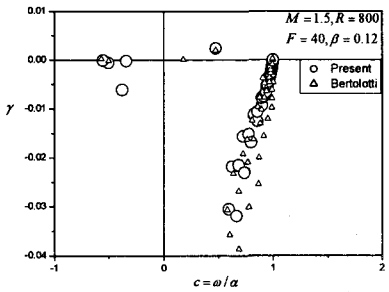

Fig.5.2 Spectrum of eigenvalues, spatial growth, parallel flow,3D disturbance.

(1) Test 1

$Mach = 1.5, \beta = 0.0, F = 40, R = 800, \ T_{stag} = 311K$

Bertolotti: $\gamma = 0.00149166, \ \omega/\alpha_r = 0.46859714$

Present: $\gamma = 0.00143199, \ \omega/\alpha_r = 0.46758739$

(2) Test 2

$Mach = 1.5, \ \beta = 0.12, \ F = 40, \ R = 800, T_{stag} = 311K$

Bertolotti: $\gamma = 0.00201235, \ \omega/\alpha_r = 0.47794974$

Present: $\gamma = 0.00279985, \ \omega/\alpha_r = 0.47257223$

(3) Test 3

$Mach = 4.5, \ \beta = 0.0, \ F = 153.3, \ R = 1500, T_{stag} = 1100K$

Malik: $\gamma = 0.00249034, \ \alpha_r = 0.25341578$

Present: $\gamma = 0.00240035, \ \alpha_r = 0.25101562$

We can find that the method of Taylor expansion is accurate to get initial unstable eigenvalues.

The PSE has a property that can recover correct

eigenvalue and eigenfunctions as the marching process proceeds downstream even if incorrect initial conditions which do not depart too much from the correct solution are given. We test this property by calculating the followiing example: $Mach = 1.5, F = 10^6 (2\pi\nu_\infty f/u_\infty^2), R = 400$. We set the mean flow is frozen(fixed for all x locations) and the mean normal velocity component is set to zero. We disturb the initial condition largely, and then carry out PSE procedure. The results are shown in Fig.5.3. It can be concluded that the PSE equations can recovery the correct solution as it marches downstream. Second, any imperfect initial conditions result in transients in the marching solution.

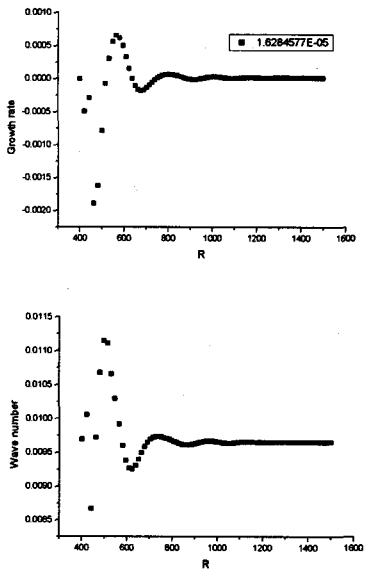

Fig.5.3. Effect of incorrect initial conditions on PSE solution for a Mach 1.5 parallel mean flow at R=400.

6 Results and Discussion

6.1 Measures of physical growth

In the parallel flow approximation, all physical quantities grow or decay according to the eigenvalue of Orr-Sommerfeld equation in exactly the same way. In nonparallel basic flow, the growth and phase variation of some physical quantity ϕ depends on α, Ψ, and possibly the y derivatives of Ψ. The physical growth rate is defined as the logarithmic derivative

$$\bar{\gamma} = \frac{1}{\phi}\frac{\partial \phi}{\partial x} \qquad (24)$$

where, the division by ϕ renders the result independent of the magnitude of ϕ. Substitution of (16) into (24) gives

$$\bar{\gamma} = \gamma - i\frac{1}{\psi}\frac{\partial \psi}{\partial x} \qquad (25)$$

$$\bar{\alpha_r} = \alpha_r - i\frac{1}{\psi}\frac{\partial \psi}{\partial x} \qquad (26)$$

Bertolotti found that the measurement of the streamwise change of u'_{max} to be a good indicator for the growth of disturbance. Measured growth data based on u'_{max} are independent of the traversed path of the sensor and avoid the need to determine the exact height of the location above the plate. Another good indicator is the maximum mass flux.

6.2 PSE results of two dimensional disturbances

In the study of three-dimensional waves we introduce the parameter

$$b = \beta \cdot 10^3 / R_0 \qquad (27)$$

which is proportional to the dimensional wave number in spanwise direction. The division by R_0 renders b independent of the reference length. The dimensional spanwise wavenumber remains constants as the TS wave is convected downstream.

Figure 6.1-6.3 display the growth rates at various Mach numbers for a two-dimensional wave at F=40 according to Bertolotti' parameters. The measurement of growth rate based on the maximum mass flux is presented. The nonparallel growth rate is larger than parallel results at M=0.02, but the situation is reversed when Mach number is increased. At M=1.0 and M=1.5, the nonparallel growth rate is smaller than the parallel results. For two-dimensional disturbances the nonparallelism seems to stabilize the flow as the Mach number is increased.

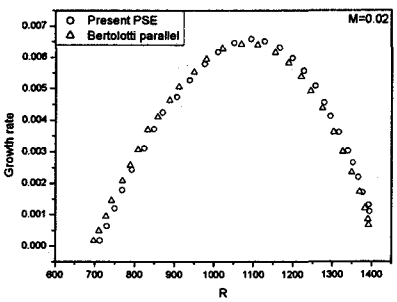

Figure 6.1 growth rates vs R at F=40,b=0, Tstag=311k, M=0.02

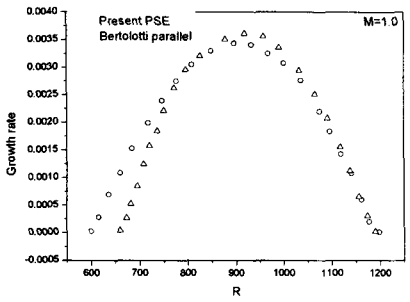

Figure 6.2 growth rates vs R at F=40,b=0, Tstag=311k, M=1.0

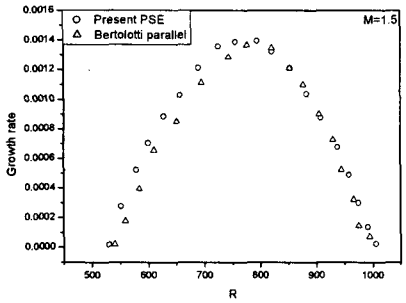

Figure 6.3 growth rates vs R at F=40,b=0,Tstag=311k, M=1.5

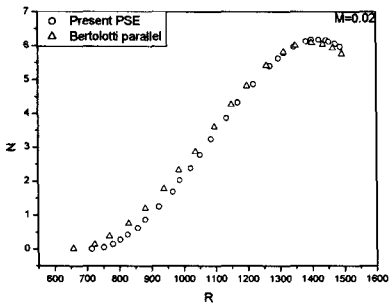

Figure 6.4 Amplitude factor vs R at F=40,b=0, Tstag=311k, M=0.02

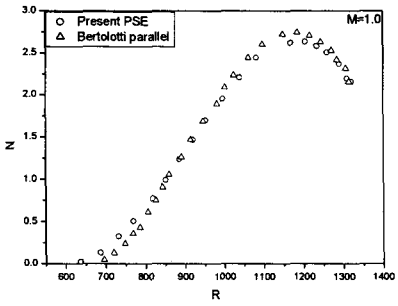

Figure 6.5 Amplitude factor vs R at F=40,b=0, Tstag=311k, M=1.0

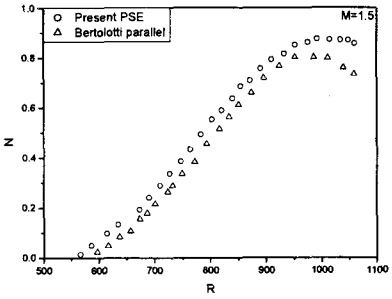

Figure 6.6 Amplitude factor vs R at F=40,b=0, Tstag=311k, M=1.5

The following figure is a comparison with the two dimensional modes reported in El-Hady&Nayfeh[10].

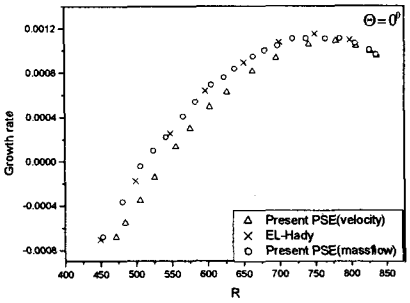

Fig.6.7 Growth rates vs R at F=40,M=1.6,Tstag=311K. Comparison with multiple scales data of EL-Hady

6.3 PSE results of three dimensional disturbance

Figures 6.8-6.9 display the growth rates at various Mach numbers for a three-dimensional wave at F=40,b=0.15 according to Bertolotti's parameters. It can be found that the effect of nonparallelism on stability is larger at three-dimensional wave than at two dimensional wave. Furthermore, the larger the Mach number, the larger the effect of the nonparallelism.

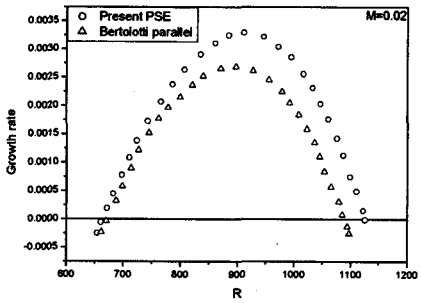

Fig.6.8 Growth rate vs R at F=40,b=0, Tstag=311k, M=0.02, b=0.15

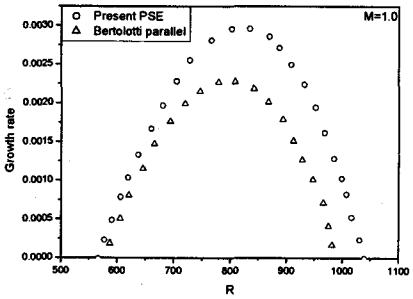

Fig.6.9 Growth rate vs R at F=40,b=0, Tstag=311k, M=1.0, b=0.15

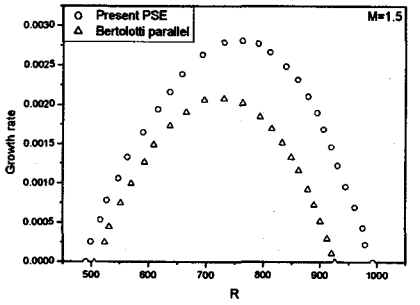

Fig.6.10 Growth rate vs R at F=40,b=0, Tstag=311k, M=1.5, b=0.15

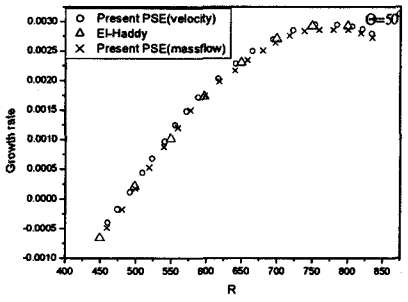

Fig.6.11 Growth rates vs R at F=40,M=1.6,Tstag=311K. Comparison with multiple scales data of EL-Hady

7 Conclusions

Linear compressible boundary layer stability is studied by using the PSE approach. The governing equations are solved by first-order backward difference for the streamwise derivatives while wall-normal direction is discretized by fourth-order difference, which uses one-side difference which does not involve the wall points to approximate the first derivative of pressure.

The effect of mean-flow nonparallelism is found to be weak on two dimensional waves and strong on three dimensional waves. As Mach number is increased, the nonparallel effect is increased. The present PSE results are in good agreement with multiple scales data.

The test of flat plate indicates that PSE is a physically meaningful tool to research stability with little computer power. The non-orthogonal coordinate system is helpful for our future work to extend PSE to complex geometries, such as hump, dip or cone at angle of attack.

ACKNOWLEDGMENT

This research was supported by the Flight vehicle Research center at Seoul National University under the sponsorship of Ministry of Defense, Korea.

References

[1] Malik,M.R.,"Stability Theory for Laminar flow Control Design." Control Design."Viscous Drag Reduction in Boundary Layers. D.M.Bushnell and J.N.Hefner.pp.3-46.

[2] D.Arnal,Description and prediction of transition two dimensional, incompressible flow. In special Course on Stability and Transition of Laminar Flows,pp 2/1-71. AGARD Report 709,1984.

[3] D. Arnal. Boundary layer transition: Predictions based on linear theory. In special Course on Progress in Transition Modelling,pp.2/1-63. AGARD reports,793,1994

[4] V.Esfahanian,K.Hejranfar. Linear and Nonlinear PSE for Stability Analysis of the Blasius Boundary Layer Using Compact Scheme. Journal of Fluids Engineering. ASME. September 2001,Vol.123/545

[5] Sean Hu and Xiaolin Zhong. Nonparallel stability Analysis of Compressible Boundary Layer using 3-D PSE. AIAA 1999

[6] C-L.Chang&M.R.Malik.Compressible Stability of Growing Boundary Layers Using Parabolized Stability Equations. AIAA 91-1636

[7] Li,F. and Malik,M.R., " On the Nature of PSE approximation," Theoretical and computational Fluid dynamics, Vol.8,1996,pp. 253-273

[8] Tuncer cebeci, Peter Bradshaw, "Physical and Computational Aspects of Convective Heat Transfer". Springer-Verlag. New York.

[9] F.P.Bertolotti, "Compressible Boundary Layer Stability analyzed with the PSE equations." AIAA-91-1637-CP

[10] F.P.Bertolotti, "Linear and nonlinear stability of boundary layers with steamwise varying properties." Phd dissertation. The Ohio State University,1991.